HHS Public Access

Author manuscript

Cancer Prev Res (Phila). Author manuscript; available in PMC 2016 September 01.

Published in final edited form as:

Cancer Prev Res (Phila). 2015 September ; 8(9): 835–844. doi:10.1158/1940-6207.CAPR-15-0051.

Chemopreventive effects of Korean Angelica vs. its major pyranocoumarins on two lineages of transgenic adenocarcinoma of mouse prostate carcinogenesis

Su-Ni Tang[1], **Jinhui Zhang**[1], **Wei Wu**[1], **Peixin Jiang**[1], **Manohar Puppala**[2], **Yong Zhang**[1], **Chengguo Xing**[2], **Sung-Hoon Kim**[3], **Cheng Jiang**[1], and **Junxuan Lü**[1,*]

[1]Department of Biomedical Sciences, Texas Tech University Health Sciences Center School of Pharmacy, Amarillo, Texas 79106, USA

[2]Department of Medicinal Chemistry, University of Minnesota, Minneapolis, MN 55455, USA

[3]Cancer Preventive Material Development Research Center, College of Oriental Medicine, Kyunghee University, Republic of Korea

Abstract

We showed previously that daily gavage of *Angelica gigas* Nakai (AGN) root ethanolic extract starting 8 weeks of age inhibited growth of prostate epithelium and neuroendocrine carcinomas (NE-Ca) in the transgenic adenocarcinoma of mouse prostate (TRAMP) model. Since decursin (D) and its isomer decursinol angelate (DA) are major pyranocoumarins in AGN extract, we tested the hypothesis that D/DA represented active/prodrug compounds against TRAMP carcinogenesis. Three groups of male C57BL/6 TRAMP mice were gavage-treated daily with excipient vehicle, AGN (5 mg per mouse) or equimolar D/DA (3 mg per mouse) from 8 weeks to 16 or 28 weeks of age. Measurement of plasma and NE-Ca D, DA and their common metabolite decursinol indicated similar retention from AGN vs. D/DA dosing. The growth of TRAMP dorsolateral prostate (DLP) in AGN-and D/DA-treated mice was inhibited by 66% and 61% at 16 weeks and by 67% and 72% at 28 weeks, respectively. Survival of mice bearing NE-Ca to 28 weeks was improved by AGN, but not by D/DA. Nevertheless, AGN-and D/DA-treated mice had lower NE-Ca burden. Immunohistochemical and mRNA analyses of DLP showed AGN and D/DA exerted similar inhibition of TRAMP epithelial lesion progression and key cell cycle genes. Profiling of NE-Ca mRNA showed a greater scope of modulating angiogenesis, epithelial-mesenchymal-transition, invasion-metastasis and inflammation genes by AGN than D/DA. The data therefore support D/DA as probable active/prodrug compounds against TRAMP epithelial lesions, and they cooperate with non-pyranocoumarin compounds to fully express AGN efficacy against NE-Ca.

Keywords

Angelica gigas Nakai; decursin; decursinol; TRAMP model; prostate cancer

[*]Corresponding Author: Junxuan Lü, Ph. D, Department of Biomedical Sciences, School of Pharmacy, Texas Tech University Health Sciences Center. 1300 S. Coulter St, Amarillo, TX 79106. Phone 1-806-414-9208, FAX 1-806-356-4643, junxuan.lu@ttuhsc.edu.

Disclosure of Potential Conflicts of Interest: All authors have no personal or financial conflict of interest and have not entered into any agreement that could interfere with our access to the data on the research or on our ability to analyze the data independently, to prepare articles, and to publish them.

Introduction

Prostate cancer (PCA) is a leading cause of cancer death in the US and Western countries. Because of the long latency period of PCA formation, chemoprevention using naturally-occurring or synthetic chemicals is considered as a plausible approach to block, delay, or even reverse carcinogenesis and progression of PCA. Herbal natural products represent a source of chemopreventive agents with desirable safety attributes and distinct targeting actions for prostate cancer chemoprevention (1). Korean Dang-gui (*Angelica gigas* Nakai, AGN) is a traditional medicinal herb used in Korea and other Asian countries (2). Its dried root extract is marketed as a dietary supplement for pain relief and memory enhancement in the United States and globally. AGN-containing multiple herbal supplements have been tested and found efficacious for relieving postmenopausal symptoms in US women (3).

Decursin (D) and its structural isomer on the side chain decursinol angelate (DA) are the major pyranocoumarin compounds of the alcoholic extract of the root of AGN (1, 2, 4) (Fig. 1A). Decursin, DA and their pyranocoumarin core decursinol (DOH) have been reported to exert neuro-protective and pain-killing activities (2). We have earlier demonstrated that in the androgen-dependent LNCaP prostate cancer cell model, ethanol extract of AGN suppressed PSA expression at both mRNA and protein levels, inhibited androgen-induced cell proliferation and blocked the ability of androgen to suppress neuroendocrine differentiation at exposure concentrations that caused G_1 arrest but far below those that induced apoptosis (5). In cell culture models, structure-activity comparison by us and others identified D and DA to have identical anti-androgen signaling and anti-proliferative activities (5, 6), whereas DOH was much less inhibitory on AR signaling, cellular growth and survival parameters in the same concentration range (5–7). We and others have shown in rodents that D and DA are rapidly and extensively converted to DOH (8–11) (Fig. 1A), and we have confirmed such extensive conversion in healthy human subjects (12).

We reported *in vivo* inhibitory effect of AGN ethanol extract on the growth of androgen-independent DU145 and PC3 PCA xenografts (11) and extended efficacy evaluation into the transgenic adenocarcinoma of mouse prostate (TRAMP) primary carcinogenesis model (13). In TRAMP mice, at least two distinct lineages of carcinogenesis exist (14–17), i.e., the androgen receptor (AR)/probasin promoter-driven SV40 antigen-mediated prostate epithelial atypical hyperplasia formation especially in the dorsal-lateral prostate (DLP), and the SV40 antigen-driven AR-independent neuroendocrine carcinomas (NE-Ca) predominantly originating in the ventral prostate (VP). In the C57BL/6 genetic background, life-time NE-Ca incidence rate was estimated to be 1/5–1/3 (14, 16, 17). Our data have shown that daily gavage administration of AGN root ethanol extract starting from 8 weeks of age to 24 weeks inhibited the growth of TRAMP DLP and NE-Ca in the TRAMP C57BL/6 mice (13). However, whether D and DA represent active/prodrug compounds against prostate primary carcinogenesis in TRAMP or any other organ sites has not been tested.

In this study, we compared the efficacy of gavage administration of AGN extract and equimolar D/DA to inhibit the two lineages of TRAMP carcinogenesis. We investigated

associated cellular and molecular changes to provide mechanistic insights into their potential differential targets.

Materials and Methods

Chemicals and Reagents

Alcoholic extract of dried AGN root was prepared by Kim's group with modification at the Oriental Medical Hospital of Kyunghee University (Seoul, Korea). Instead of manual extraction (5, 13), bulk extraction of powdered AGN root was carried out in a hospital herbal pharmacy extractor with 95% hot alcohol. Chemical fingerprinting of AGN by HPLC-UV showed that content of D plus DA in AGN extract was 60%. Since D and DA possess identical anti-AR, anti-proliferative and apoptotic cellular activities (5, 6, 18), and their majority is converted to DOH (8–11), they were isolated together as a mixture by Xing's group at University of Minnesota. The purity of D/DA was > 99% based on monitoring with NMR and HPLC.

Mayer's hematoxylin was obtained from Sigma-Aldrich (St. Louis, MO) and eosin Y was purchased from Thermo Fisher Scientific (Pittsburgh, PA). SV40-T antigen (T-Ag), androgen receptor (AR) and synaptophysin antibodies were purchased from BD Pharmingen (San Diego, CA), EMD Millipore (Billerica, MA) and BD Transduction Laboratories (San Diego, CA), respectively. PCR primers were purchased from Integrated DNA Technologies, Inc. (Coralville, IA).

Animal experiment

The animal study was approved by the IACUC of Texas Tech University Health Sciences Center and carried out on the Amarillo campus. TRAMP mice were bred in-house and identified per genotyping protocol as reported before (16, 17). Male C57BL/6 TRAMP mice and their male wild type (WT) littermates were used. Cohorts of male TRAMP mice (35–36 mice per group) were fed AIN93M purified diet and gavage-treated with 0.15 mL excipient vehicle (ethanol: PEG400: Tween 80: 5% glucose = 3:6:1:20), AGN (5 mg per mouse) or D/DA (3 mg per mouse, equimolar to that in AGN) 5 days per week from 8 weeks of age. Fifteen WT littermates were enrolled and treated with vehicle only to serve as the baseline reference for TRAMP prostate lobe expansion. Animals were weighed weekly. Starting 16 weeks, TRAMP mice were palpated for abdominal mass indicative of prostate/genito-urinary (GU) tumors. Mice were euthanized at either 16 weeks (n ~11–13 TRAMP mice per group and n=6 for WT littermates) or 28 weeks unless large tumors necessitated earlier sacrifice.

Blood was taken by cardiac puncture after anesthesia sedation at 3 h after the last dose. At necropsy, the GU tract was removed *en bloc* and weighed. Tumors were dissected and weighed. The pelvic lymph nodes were inspected for enlargement (metastasis) and, if visible, were dissected, weighed, and fixed in 10% neutral buffered formalin for hematoxylin and eosin (H&E) and immunohistochemical (IHC) confirmation of metastasis. The prostate from mice without visible tumors were carefully dissected into anterior prostate (AP), dorsolateral prostate (DLP), and ventral prostate (VP) and weighed. Left lobes from

each mouse were fixed in 10% neutral buffered formalin for H&E and IHC pathology analyses. Right lobes were snap frozen on dry ice and stored at −80°C for biochemical and molecular biomarkers analyses. Liver and kidney were inspected for health problems, dissected, weighed and preserved for later analyses.

Analysis of D, DA and DOH in mouse plasma and NE-Ca

The D, DA and DOH levels in plasma were analyzed on an Agilent Infinity 1260 HPLC system by our validated procedure as described before (8). D, DA and DOH levels in tumor tissues were determined by a Shimadzu Nexera UHPLC system coupled to an AB Sciex 5500 QTRAP MS/MS detector per our validated procedure (9, 19). To extract D, DA and DOH from tumor tissue, a piece of frozen tumor was homogenized in 4 volumes of water by using a tissue homogenizer. The tumor homogenate (200 μL, equivalent to 50 mg tumor) was then spiked with prednisolone (5 ng, IS) and extracted with ethyl acetate as for plasma samples.

Histology and IHC analyses

Formalin-fixed prostate lobes were processed and embedded in paraffin and routinely stained by H&E as we previously reported (16, 17). For IHC, 5-μm sections were mounted onto adhesive microscope slides. Tissue sections were deparaffinized in xylenes and rehydrated in a series of decreasing concentrations of ethanol. Tissue sections were then heated in 10 mM citrate buffer solution for antigen retrieval. After sections were rinsed in distilled water, 3% hydrogen peroxide was used for quenching. After incubating with normal serum for 30 minutes, sections were applied with primary and secondary antibodies according to manufacturer's instructions. The slides were developed in diaminobenzidine and counterstained with a weak solution of hematoxylin stain. The stained slides were dehydrated and mounted in Permount. Synaptophysin (NE-Ca), AR (epithelial) expression in all tumors were detected to confirm NE-Ca diagnoses as reported before (16, 17). See Supplement Fig. S1 for illustrative examples of H&E and IHC characterization.

Scoring of prostate lesions

Mouse prostatic tumors or lobes from TRAMP mice were characterized by H&E and TAg staining. Prostatic lesions were scored according to our composite scoring scheme adapted and modified based on that of Suttie and colleagues (20) (see Supplement Fig. S2 for description). In brief, severity of epithelial lesions was divided into 5 grades: mild lesions as grade I, moderate lesions as grade II, severe lesions as grade III-IV, and adenoma as grade V. The lesion grade was modified by their distribution patterns as focal, multifocal or diffuse. Therefore scores for grade I lesions ranged from 1–3, and likewise for grade V ranged from 13–15. For each lobe, the most severe lesion and its distribution pattern were used to derive the lesion score.

DLP and NE-Ca tissue sampling, RNA extraction and Real-time RT-PCR for expression of selected genes

Due to limited amount of DLP tissue available from each mouse, we pooled them by group into a sample for RNA extraction and qRT-PCR analyses of genes known to be involved in

TRAMP epithelial cell cycle regulation. For NE-Ca, we analyzed 4 IHC-confirmed NE-Ca per group of TRAMP mice treated with vehicle, AGN vs. D/DA, respectively. Total RNA was prepared from 30 mg of NE-Ca tissues using the AllPrep DNA/RNA/Protein Mini kit (QIAGEN Inc., Valencia, CA) (21, 22). RNA (1 μg) was used for cDNA synthesis by using the iScript cDNA synthesis kit (Bio-Rad Laboratories, Inc., Hercules, CA) according to the manufacturer's instructions. qRT-PCR was performed by using the Fast Start Universal SYBR Master with ROX (Hoffmann-La Roche Ltd., Basel, Switzerland) on the CFX96 Touch Real-Time PCR Detection Systems (Bio-Rad Laboratories, Inc., Hercules, CA). All reactions were performed in duplicate, and the relative expression of target mRNA in each sample was normalized with that of mean β-actin. The sequences of these primers were as listed in Supplement Table S1.

Statistical analysis

The mean and SD were calculated for each experimental group. Differences among groups were analyzed by one or two way ANOVA using PRISM statistical analysis software, when the data distribution conformed to normality and homogeneity requirements (GraphPad Software, Inc., La Jolla, CA). For comparison involving only two groups, Student's t-test was used. Significant differences were calculated at $P<0.05$.

Results

Gavage treatment with AGN and equimolar D/DA led to similar DOH levels in mouse plasma or tumor

It is now well established that D and DA are extensively converted to DOH in rodents (8–11, 19) (Fig. 1A). We therefore tested whether daily gavage administration of AGN extract and equimolar D/DA to TRAMP mice led to similar uptake and retention by measuring D, DA and DOH levels in 8 plasma samples at 16 and 28 weeks of age and 4 tumors collected from each treatment group at 28 weeks. Fig. 1B shows representative chromatograms of separating DOH from D and DA of a NE-Ca sample by LC-MS/MS detection. Data in Fig. 1C showed no statistical difference between the plasma DOH concentration of AGN- and D/DA-treated mice at 16 weeks ($p = 0.199$) and at 28 weeks ($p = 0.858$), whereas the D and DA levels were below the level of detection of the UV diode detector. The trend for higher plasma DOH at 28 weeks (2921, 3076 ng/ml) vs. 16 weeks (1592, 1927 ng/ml) likely reflected rising trough level after repeated dosing. Similarly, the NE-Ca DOH content was not statistically different between AGN- and D/DA-treated groups (2078 ng/g vs. 2573 ng/g, $p > 0.05$) (Fig. 1C). As expected, the D and DA content in the NE-Ca were much lower than DOH (Fig. 1B, note the different mass intensity scales for DOH vs. D and DA); and they were not statistically different between AGN-treated and D/DA-treated group (Fig. 1C). Therefore, our data indicated that other phytochemicals in AGN did not affect the metabolic fate of D and DA and the consumption of AGN extract and equimolar purified D/DA resulted in similar, if not identical, bioavailability of D/DA and their conversion to DOH.

AGN and D/DA treatment did not affect body weight or organ weight of TRAMP mice

At the daily gavage dose of 5 mg AGN and 3 mg D/DA, the body weight of the TRAMP mice was the same as the vehicle-treated TRAMP mice in the 16-week cohort (Fig. 2A). For

the 28-week cohort, the body weight of the 3 groups of TRAMP mice remained same for up to 18 weeks and then displayed some variation from large NE-Ca in some TRAMP mice (Fig. 2B). The vehicle-treated wild type (WT) mice weighed 2–3 grams more than the TRAMP mice in the 16-week cohort due in part to weight advantage at assignment at 8 weeks (Fig. 2A). In the 28-week cohorts (Fig. 2B), the WT mice had some growth advantage over the TRAMP mice, especially at 24 weeks or older when the large NE-Ca negatively affected health of some TRAMP mice. Normalized to body weight, major organs involved in D/DA metabolism to DOH (liver) (10, 19) and DOH clearance (kidney) were not different among the AGN, D/DA and vehicle groups (Fig. 2C, D). Overall, the data were consistent with our earlier studies in xenograft models (11) and TRAMP model (13) of the well tolerated nature of AGN, and D/DA.

Gavage with AGN and D/DA exerted the same extent of inhibition of TRAMP dorsolateral prostate epithelial lesions

Since DLP is the most expanded lobe in TRAMP mouse prostate (23) and the anatomical site where atypical hyperplastic epithelial lesions mostly arise (14, 17, 23), we compared DLP weight of the TRAMP mice treated with vehicle, AGN or D/DA with that of the wild type (WT) mice. As shown in Fig. 3A and B, the TRAMP DLP expansion was 2 fold and 3 fold, respectively, over the WT baseline by 16 and 28 weeks of age. The AGN- and D/DA-treated TRAMP mice showed 66% and 61% respective normalization of the DLP weight at 16 weeks (Fig. 3A). At 28 weeks, the inhibition of TRAMP DLP growth by AGN and D/DA was 67% and 72%, respectively (Fig. 3B). The sum weight of the AP, DLP and VP lobes (total prostrate) showed same overall suppression by AGN and D/DA at 16 and 28 weeks (Fig. 3C and 3D), albeit less as dramatic as in DLP in part due to the AP growth was not significantly decreased by AGN or D/DA (Supplement Table S2). The VP, smallest of the 3 lobes, expanded to a much less extent than the DLP, and AGN and D/DA suppressed the TRAMP VP growth to similar percentage as in DLP (Supplement Table S2).

We next examined the effects of AGN and D/DA on the histopathology of the epithelial lesions in TRAMP DLP. The DLP lobes (from WT and TRAMP) were stained with T-Ag antibody to locate the areas of epithelial lesions (Fig. 4A, and see Supplement Fig. S1A for H&E and IHC verification). WT mouse prostates, as usual, showed negative signal of T-Ag in epithelial cells. The epithelial T-Ag and AR IHC staining (data not shown) was not different among the TRAMP groups. We scored the most severe lesions using a composite scoring scheme (Supplement Fig. S2) taking into consideration of the lesion grade (mild hyperplasia to adenoma) and their distribution patterns (focal, multi-focal or diffuse). The score range was: 1 = focal mild hyperplasia to 15 = diffuse adenoma. From 16 to 28 weeks, the mean lesion score of DLP increased from 7.9 to 11.1 in TRAMP vehicle mice (Fig. 4B). AGN extract significantly decreased the mean lesion score of DLP from 7.9 to 6.2 ($P<0.05$) by 16 weeks and from 11.1 to 7.9 ($P < 0.001$) by 28 weeks (Fig. 4B). Similarly, D/DA also reduced the mean lesion score of DLP to 7.2 ($P < 0.001$) by 28 weeks (Fig. 4B). The progression of DLP epithelial lesions was retarded sufficiently by both AGN extract and D/DA in TRAMP DLP so that their lesions at 28 weeks resembled those in the vehicle-treated TRAMP mice at 16 weeks (Fig. 4B).

AGN and D/DA treatment decreased TRAMP DLP proliferation and key cell cycle genes

Because TRAMP epithelial lesions are principally driven by increased cellular proliferation, we examined the effect of AGN and D/DA treatments on Ki-67 proliferation biomarker. As shown is Fig. 4A, Ki-67 was highly expressed in some but not all T-Ag+ cells in TRAMP mouse DLP. AGN extract or D/DA decreased Ki-67 staining (Fig. 4A). Due to the small amount of DLP tissues, we analyzed pooled samples from each group for the mRNA expression level of key genes known to be involved in the proliferation of TRAMP epithelial lesions such as *Pcna*, *p21Cip1*, *p16ink4a*, *cyclin A2(Ccna2)* (24, 25) (Fig. 4C). Whereas the vehicle-treated TRAMP mice showed elevated expression of all these genes compared to WT DLP (set as unity), AGN and D/DA treatment resulted in the same extent of attenuation of their expressions (Fig. 4C). Taken together, these results demonstrated AGN extract and equimolar D/DA exerted same and profound inhibitory effect on DLP epithelial lesions as reflected by decreased lesion score/severity, attenuated expression of cell cycle and proliferative genes and lower Ki-67 staining, cumulating to decreased TRAMP DLP prostate lobe weight.

AGN exerted greater inhibition of growth of NE-Ca than equimolar D/DA

The aggressive growth nature of TRAMP NE-Ca (all verified by IHC staining for positive T-Ag, positive synaptophysin, and negative AR, Supplement Fig. S1A) necessitated euthanasia as early as 19 weeks of age for vehicle-treated TRAMP mice and 5 mice were sacrificed with NE-Ca weighing 7–10 grams before the planned experiment terminal endpoint of 28 weeks (Fig. 5A and B). By 28 weeks, the incidence of dissectible prostate NE-Ca was as follows: vehicle group 7/20 (35%), AGN group 6/21 (29%) and D/DA group 8/22 (36%) (Fig. 5A; Supplement Fig S1C). The observed NE-Ca incidence rate was in agreement with previous findings of us and others that the life time incidence of NE-Ca in C57B/6 background is ~1/3 (14, 16, 17). Whereas neither AGN nor D/DA decreased the cumulative incidence of NE-Ca by 28 week endpoint (Fig. 5A), only 2 AGN-treated TRAMP mice needed euthanasia before this time, with tumors weighing 4–5 grams (Fig. 5B, squares). However, the euthanasia rate (6/22 enrolled mice) for D/DA-treated TRAMP mice before 28 weeks was comparable to the vehicle group (5/20 enrolled mice) (Fig. 5B, triangle vs. circles). Thus, AGN prolonged survival of mice bearing NE-Ca (Fig. 5C) with the smallest cancer burden overall (Fig. 5D). In comparison, D/DA did not have a survival advantage for NE-Ca bearing mice (Fig. 5C), but decreased the cancer burden when compared to the vehicle-treated counterparts (Fig. 5D).

AGN decreased incidence of metastatic lymph nodes

AGN decreased metastasis of NE-Ca to pelvic lymph nodes as verified by IHC (i.e., 3/6 for AGN-treated, NE-Ca bearing mice; vs. 7/7 for vehicle-treated NE-Ca bearing mice (Fig. 5A) (Supplement Fig. S1B, C). The size of the metastatic lymph nodes was smaller for AGN-treated (average weight 53 mg) TRAMP mice than in the vehicle-treated TRAMP mice (average weight 107 mg) (Supplement Fig. S1C). Whereas the incidence of metastatic lymph node for D/DA-treated TRAMP mice (3/8, Fig. 5A) and average lymph node weight (34 mg, Supplement Fig. S1C) were lower than the vehicle-treated TRAMP mice, data

interpretation was confounded by the smaller NE-Ca size when the D/DA-treated, NE-Ca bearing TRAMP mice had to be euthanized (Fig. 5B).

Targeted gene expression profiling by qRT-PCR analyses of mRNA from NE-Ca

To seek molecular insights into the differential NE-Ca inhibition efficacy of AGN vs. D/DA, we did targeted profiling of the steady state mRNA for gene expression patterns in 4 NE-Ca from each group. The choice of genes was based on our earlier report of integrated "omic" profiling of NE-Ca treated with AGN (13), focusing on cell proliferation, angiogenesis (*Fgf* axis and *Vegf* axis), epithelial-mesenchymal transition (EMT)/metastasis and inflammation (Table 1). As a well-recognized cellular proliferation biomarker, NE-Ca *Pcna* was lower in AGN- and D/DA-treated mice, with respective suppression of 61% and. 49%. Flap endonuclease 1 (*Fen1*), an endonuclease that complexes with PCNA in DNA repair (26, 27), was suppressed by AGN and D/DA by 53% and 47%. *Stat3*, another known proliferation signaling molecule for TRAMP NE-Ca growth (28), was suppressed 73% and 52% by AGN and D/DA, respectively. The differential attenuation of the expression levels of these proliferation molecules roughly correlated with the NE-Ca growth inhibiting efficacy parameters by AGN and D/DA.

Synaptotagmin IV (*Syt4*), a gene related to neuro synaptic signaling (29), was suppressed by 94% and 84% in AGN and D/DA-treated NE-Ca, respectively. *Sox5*, a gene involved in neurogenesis and patterning (30, 31), was 56% lower in AGN- and D/DA-treated NE-Ca than the vehicle-treated counterpart. These genes reflected the neuroendocrine lineage of the analyzed NE-Ca samples. For angiogenesis-related genes, both AGN and D/DA treatment decreased *Fgf10*, *Mmp2* and *Fgfbp3* (*Fgf* axis), yet AGN, but not D/DA, suppressed *Vegf* and one of its receptors, *Flt1* and *Nos2*, which is known to be stimulated by VEGF in vascular endothelium (*Vegf* axis). For key EMT/metastasis/invasion genes, AGN suppressed *Snai2* (32), *Twist1* (33, 34), *Notch1* (35), *Tgfbr2* (36) and macrophage *Mmp12* whereas D/DA only suppressed *Snai2*. In favor of broader targeting of EMT regulators by AGN over D/DA, AGN increased E-cadherin expression by 2.3 fold, whereas D/DA failed. Another prostate epithelium-specific protein, ventral prostate predominant 1 (*Vpp1*), which is known to be extremely suppressed in TRAMP NE-Ca (37), was more dramatically induced by AGN (30 fold) than D/DA (19 fold). These changes indicated a greater reversal of EMT/metastasis in the AGN-treated NE-Ca than in D/DA-counterparts. In terms of inflammation related genes, AGN and D/DA suppressed to the same extent mast cell chymase 1 (*Cma1*) (~70%) and interleukin 6 signal transducer (*Il6st*), but AGN out-performed D/DA on two other mast cell genes, mast cell carboxypeptidases A3 (*Cpa3*) and mast cell protease 6 (*Mcpt6*). Furthermore, AGN, but not D/DA, suppressed *Rela* (NF-κB related). Therefore, these AGN-specific "targeted" genes could be important to contribute to the greater NE-Ca growth inhibitory efficacy and survival benefit of AGN over D/DA.

Discussion

Our present study not only confirmed the inhibitory efficacy of AGN root extract on two distinct carcinogenesis lineages in TRAMP mice (13), but also significantly extended the mechanistic insight with aspect to the "active chemicals" for each lineage. In spite of

different batches of AGN (D/DA varied ~2 fold) and excipients (Tween-80 vs. complex formulation) and different localities of the experimentation (Minnesota vs. Texas) and different lab personnel delivering treatments, AGN exerted unequivocal inhibition of the DLP epithelial lesion growth in both experiments. An additional experiment has also confirmed the TRAMP epithelial lesion suppression efficacy and dose-dependency of D/DA (Wu, Tang and Lü, unpublished data). The present work identified D/DA as active/prodrug compounds for inhibiting the epithelial lineage of TRAMP carcinogenesis. Our data from TRAMP mice (majority without NE-Ca) strongly supported that D/DA recapitulated AGN's inhibitory efficacy on the epithelial lesion growth (DLP lobe weight, total prostate weight, Fig. 3) as well as by morphological assessment of the lesion severity and molecular marker profiling (Fig. 4). As D/DA are rapidly and extensively converted to DOH in rodents (8–11) and in humans (12), future studies will need to address whether and how DOH (or its further metabolites, if any) mediate the epithelial lesion inhibitory effect. Since human prostate carcinogenesis is believed to originate from prostatic intraepithelial neoplasia (PIN) and progress to aggressive adenocarcinoma over decades, we believe the demonstrated ability of D/DA as prodrugs in the TRAMP model to inhibit the epithelial lineage lesion growth and progression is significant for extending the research into additional clinically more relevant prostate carcinogenesis models to assess the translatability into human PCa risk reduction in the future.

Regarding NE-carcinogenesis lineage, the impact of AGN was consistent across 2 experiments, resulting in inhibition of their growth and decreased the NE-Ca burden of TRAMP mice carrying them and improved their survival to the respective specified termination endpoints ((13) and Fig. 5). Our data on NE-Ca with respect to D/DA indicated measurable inhibition on their growth that was not sufficient enough to improve the survival of mice bearing NE-Ca (Fig. 5). The data suggest that non-pyranocoumarin components in AGN might not only provide cancer suppressing activity but also sustain host survival benefit to NE-Ca bearing mice alone or by cooperating with D/DA or DOH. Analyses of plasma DOH in AGN- vs. D/DA-treated mice revealed same level of DOH with non-detectable D/DA (Fig. 1C), and therefore indicated that the non-pyranocoumarin components (yet to be identified) would not alter D/DA bioavailability or conversion to DOH as a mechanism to account for the greater anti-cancer efficacy of the AGN extract over D/DA. This was consistent with our early report of no observable PK difference in rats when purified D/DA was dosed at an equimolar dose with that in AGN (9). Our preliminary profiling of mRNA levels of select genes involved in TRAMP NE-Ca angiogenesis, EMT, invasion-metastasis and inflammation further support the greater scope of "targeting" by AGN than by D/DA (Table 1). Whereas AGN decreased both *Fgf*-axis and *Vegf*-axis of angiogenesis (e.g., *Fgf10*, *Fgfbp3*, *Vegf* and *Flt1*/*Vegfr*), D/DA appeared to only affect the *Fgf*-axis without affecting the *Vegf*-axis (Table 1). For EMT-invasion-metastasis genes, AGN and D/DA affected *Snai2* in common, but AGN affected additional and more critical regulators of EMT such as *Twist*, a known master EMT regulator (33, 34), *Notch1* (35), *Tgfbr2* and E-cadherin. Since chronic inflammation is recognized to be an important contributor to cancer progression and metastasis, our profiling data indicated again the superiority of AGN over D/DA in that 3 of 5 profiled genes were suppressed to a greater extent by AGN (Table 1). In the future, we will attempt to identify the non-pyranocoumarin

components and validate their efficacy for inhibiting NE-Ca growth and improve survival of tumor-bearing mice. Beside the scientific values, these mechanistic insights will help to refine the use of AGN or D/DA/DOH as dietary supplements.

Given the impressive suppression efficacy of AGN on TRAMP carcinogenesis lineages, it is prudent here to speculate on human dose equivalent of AGN or D/DA by allometric extrapolation. The effective AGN dose of 5 mg per mouse (~200 mg/kg) would translate to 17 mg/kg for humans based on body surface area (38). Assume average adult male body weight of 70 kg, the daily human intake will be 1167 mg. AGN dietary supplements are currently marketed with recommended dosage of 800 mg daily (e.g., CognI. Q from Quality of Life Laboratories, Purchase, NY) (12). Therefore, the dosage for effective anti-epithelial and anti-cancer efficacies should be achievable in humans. Furthermore, our recently completed PK study in 20 healthy human subjects recapitulated D/DA to DOH conversion in pattern and extent as the rodent models (12), providing strong justification of the relevance of the rodent models for efficacy and mechanism studies for translation to humans.

Supplementary Material

Refer to Web version on PubMed Central for supplementary material.

Acknowledgments

Grant supports: National Center for Complementary and Integrative Health (NCCIH) grants R01AT007395 (Lü, Xing) and R21AT005383 (Lü) and National Cancer Institute grant R01 CA136953 (Lü).

The authors thank TTUHSC Animal care staff for excellent assistance with mouse breeding and care, and Dr. Li Li for guidance on pyranocoumarin analyses.

Abbreviations

AGN	*Angelica gigas* Nakai
D	Decursin
DOH	Decursinol
DA	Decursinol angelate
NE-Ca	Neuroendocrine carcinoma
TRAMP	Transgenic adenocarcinoma of mouse prostate
AP	Anterior prostate
DLP	Dorsolateral prostate
VP	Ventral Prostate

References

1. Lu J, Kim SH, Jiang C, Lee H, Guo J. Oriental herbs as a source of novel anti-androgen and prostate cancer chemopreventive agents. Acta Pharmacol Sin. 2007; 28:1365–72. [PubMed: 17723170]

2. Zhang J, Li L, Jiang C, Xing C, Kim SH, Lu J. Anti-cancer and Other Bioactivities of Korean Angelica gigas Nakai (AGN) and Its Major Pyranocoumarin Compounds. Anti-cancer agents in medicinal chemistry. 2012; 12:1239–54. [PubMed: 22583405]

3. Chang A, Kwak BY, Yi K, Kim JS. The effect of herbal extract (EstroG-100) on pre-, peri- and post-menopausal women: a randomized double-blind, placebo-controlled study. Phytotherapy research : PTR. 2012; 26:510–6. [PubMed: 21887807]

4. Ahn MJ, Lee MK, Kim YC, Sung SH. The simultaneous determination of coumarins in Angelica gigas root by high performance liquid chromatography-diode array detector coupled with electrospray ionization/mass spectrometry. J Pharm Biomed Anal. 2008; 46:258–66. [PubMed: 17997069]

5. Jiang C, Lee HJ, Li GX, Guo JM, Malewicz B, Zhao Y, et al. Potent antiandrogen and androgen receptor activities of an Angelica gigas-containing herbal formulation: Identification of decursin as a novel and active compound with implications for prevention and treatment of prostate cancer. Cancer research. 2006; 66:453–63. [PubMed: 16397261]

6. Guo J, Jiang C, Wang Z, Lee HJ, Hu H, Malewicz B, et al. A novel class of pyranocoumarin anti-androgen receptor signaling compounds. Mol Cancer Ther. 2007; 6:907–17. [PubMed: 17363485]

7. Yim D, Singh RP, Agarwal C, Lee S, Chi H, Agarwal R. A novel anticancer agent, decursin, induces G(1) arrest and apoptosis in human prostate carcinoma cells. Cancer research. 2005; 65:1035–44. [PubMed: 15705905]

8. Li L, Zhang J, Shaik AA, Zhang Y, Wang L, Xing C, et al. Quantitative Determination of Decursin, Decursinol Angelate, and Decursinol in Mouse Plasma and Tumor Tissue Using Liquid-Liquid Extraction and HPLC. Planta medica. 2012; 78:252–9. [PubMed: 22116603]

9. Li L, Zhang J, Xing C, Kim SH, Lu J. Single Oral Dose Pharmacokinetics of Decursin, Decursinol Angelate, and Decursinol in Rats. Planta medica. 2013; 79:275–80. [PubMed: 23364885]

10. Park HS, Kim B, Oh JH, Kim YC, Lee YJ. First-pass metabolism of decursin, a bioactive compound of Angelica gigas, in rats. Planta medica. 2012; 78:909–13. [PubMed: 22573368]

11. Lee HJ, Lee EO, Lee JH, Lee KS, Kim KH, Kim SH, et al. In vivo anti-cancer activity of Korean Angelica gigas and its major pyranocoumarin decursin. Am J Chin Med. 2009; 37:127–42. [PubMed: 19222117]

12. Zhang J, Li L, Hale TW, Chee W, Xing C, Jiang C, et al. Single oral dose pharmacokinetics of decursin and decursinol angelate in healthy adult men and women. PLOS One. 2015; 10:e0114992. [PubMed: 25695490]

13. Zhang J, Wang L, Zhang Y, Li L, Tang S, Xing C, et al. Chemopreventive effect of Korean Angelica root extract on TRAMP carcinogenesis and integrative “omic” profiling of affected neuroendocrine carcinomas. Molecular carcinogenesis. 2014 Epub 2014/10/14.

14. Chiaverotti T, Couto SS, Donjacour A, Mao JH, Nagase H, Cardiff RD, et al. Dissociation of epithelial and neuroendocrine carcinoma lineages in the transgenic adenocarcinoma of mouse prostate model of prostate cancer. Am J Pathol. 2008; 172:236–46. [PubMed: 18156212]

15. Huss WJ, Gray DR, Tavakoli K, Marmillion ME, Durham LE, Johnson MA, et al. Origin of androgen-insensitive poorly differentiated tumors in the transgenic adenocarcinoma of mouse prostate model. Neoplasia. 2007; 9:938–50. [PubMed: 18030362]

16. Wang L, Bonorden MJ, Li GX, Lee HJ, Hu H, Zhang Y, et al. Methyl-selenium compounds inhibit prostate carcinogenesis in the transgenic adenocarcinoma of mouse prostate model with survival benefit. Cancer Prevention Research. 2009; 2:484–95. [PubMed: 19401524]

17. Wang L, Zhang J, Zhang Y, Nkhata K, Quealy E, Liao JD, et al. Lobe-specific lineages of carcinogenesis in the transgenic adenocarcinoma of mouse prostate and their responses to chemopreventive selenium. The Prostate. 2011; 71:1429–40. [PubMed: 21360561]

18. Jiang C, Guo J, Wang Z, Xiao B, Lee HJ, Lee EO, et al. Decursin and decursinol angelate inhibit estrogen-stimulated and estrogen-independent growth and survival of breast cancer cells. Breast Cancer Res. 2007; 9:R77. [PubMed: 17986353]

19. Li L, Zhang J, Xing C, Kim SH, Jiang C, Lu J. In vitro metabolism of pyranocoumarin isomers decursin and decursinol angelate by liver microsomes from man and rodents. Planta medica. 2013; 79:1536–44. [PubMed: 24026903]

20. Suttie A, Nyska A, Haseman JK, Moser GJ, Hackett TR, Goldsworthy TL. A grading scheme for the assessment of proliferative lesions of the mouse prostate in the TRAMP model. Toxicologic pathology. 2003; 31:31–8. [PubMed: 12597447]
21. Zhang J, Nkhata K, Shaik AA, Wang L, Li L, Zhang Y, et al. Mouse prostate proteome changes induced by oral pentagalloylglucose treatment suggest targets for cancer chemoprevention. Current cancer drug targets. 2011; 11:787–98. [PubMed: 21762084]
22. Zhang J, Wang L, Li G, Anderson LB, Xu Y, Witthuhn B, et al. Mouse prostate proteomes are differentially altered by supranutritional intake of four selenium compounds. Nutrition and cancer. 2011; 63:778–89. [PubMed: 21614726]
23. Greenberg NM, DeMayo F, Finegold MJ, Medina D, Tilley WD, Aspinall JO, et al. Prostate cancer in a transgenic mouse. Proceedings of the National Academy of Sciences of the United States of America. 1995; 92:3439–43. [PubMed: 7724580]
24. Zhang J, Wang L, Zhang Y, Li L, Higgins L, Lu J. Lobe-specific proteome changes in the dorsal-lateral and ventral prostate of TRAMP mice versus wild-type mice. Proteomics. 2011; 11:2542–9. [PubMed: 21598396]
25. Zhang, J.; Wang, L.; Zhang, Y.; Lü, J. Lobe-Specific Carcinogenesis in the Transgenic Adenocarcinoma of Mouse Prostate (TRAMP) Mouse Model. In: Tonissen, Kathryn, editor. InTech. 2013. Carcinogenesis
26. Li X, Li J, Harrington J, Lieber MR, Burgers PM. Lagging strand DNA synthesis at the eukaryotic replication fork involves binding and stimulation of FEN-1 by proliferating cell nuclear antigen. The Journal of biological chemistry. 1995; 270:22109–12. [PubMed: 7673186]
27. Balakrishnan L, Bambara RA. Flap endonuclease 1. Annual review of biochemistry. 2013; 82:119–38.
28. Hafeez BB, Zhong W, Mustafa A, Fischer JW, Witkowsky O, Verma AK. Plumbagin inhibits prostate cancer development in TRAMP mice via targeting PKCepsilon, Stat3 and neuroendocrine markers. Carcinogenesis. 2012; 33:2586–92. [PubMed: 22976928]
29. Xi D, Chin H, Gainer H. Analysis of synaptotagmin I-IV messenger RNA expression and developmental regulation in the rat hypothalamus and pituitary. Neuroscience. 1999; 88:425–35. [PubMed: 10197764]
30. Perez-Alcala S, Nieto MA, Barbas JA. LSox5 regulates RhoB expression in the neural tube and promotes generation of the neural crest. Development. 2004; 131:4455–65. [PubMed: 15306568]
31. Stolt CC, Schlierf A, Lommes P, Hillgartner S, Werner T, Kosian T, et al. SoxD proteins influence multiple stages of oligodendrocyte development and modulate SoxE protein function. Developmental cell. 2006; 11:697–709. [PubMed: 17084361]
32. Alves CC, Carneiro F, Hoefler H, Becker KF. Role of the epithelial-mesenchymal transition regulator Slug in primary human cancers. Front Biosci (Landmark Ed). 2009; 14:3035–50. [PubMed: 19273255]
33. Yang J, Mani SA, Donaher JL, Ramaswamy S, Itzykson RA, Come C, et al. Twist, a master regulator of morphogenesis, plays an essential role in tumor metastasis. Cell. 2004; 117:927–39. [PubMed: 15210113]
34. Yang J, Mani SA, Weinberg RA. Exploring a new twist on tumor metastasis. Cancer research. 2006; 66:4549–52. [PubMed: 16651402]
35. Timmerman LA, Grego-Bessa J, Raya A, Bertran E, Perez-Pomares JM, Diez J, et al. Notch promotes epithelial-mesenchymal transition during cardiac development and oncogenic transformation. Genes & development. 2004; 18:99–115. [PubMed: 14701881]
36. Ding Z, Wu CJ, Chu GC, Xiao Y, Ho D, Zhang J, et al. SMAD4-dependent barrier constrains prostate cancer growth and metastatic progression. Nature. 2011; 470:269–73. [PubMed: 21289624]
37. Wubah JA, Fischer CM, Rolfzen LN, Khalili M, Kang J, Green JE, et al. Ventral prostate predominant l, a novel mouse gene expressed exclusively in the prostate. The Prostate. 2002; 51:21–9. [PubMed: 11920954]
38. Sharma V, McNeill JH. To scale or not to scale: the principles of dose extrapolation. British journal of pharmacology. 2009; 157:907–21. [PubMed: 19508398]

A. Chemical structures of major pyranocoumarins in AGN

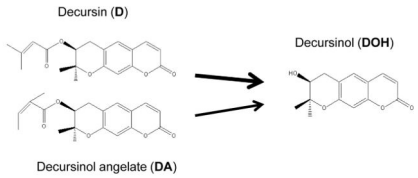

B. Representative UHPLC-MS separation of pyranocoumarins in a NE-Ca sample

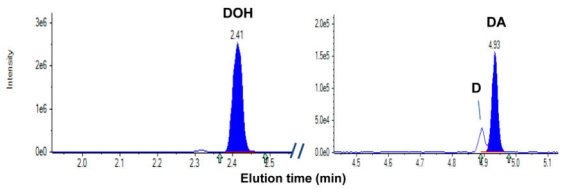

C. Pyranocoumarins in plasma and NE-Ca of TRAMP mice

Gavage cohort	Age weeks	Analyzed tissue	n	DOH ng/mL or ng/g	D ng/g	DA ng/g
AGN	16	Plasma	8	1590 ± 410	0*	0*
D/DA	16	Plasma	8	1927 ± 573	0*	0*
AGN	28	Plasma	8	3076 ± 2076	0*	0*
D/DA	28	Plasma	8	2920 ± 1202	0*	0*
AGN	28	NE-Ca	4	2078 ± 1420	8.0 ± 7.1	53.8 ± 52.2
D/DA	28	NE-Ca	4	2573 ± 1720	35.3 ± 40.5	66.3 ± 51.6

Mean ± SD. *below detection limit of HPLC-UV.

Figure 1.

Comparison of pyranocoumarin compounds in mouse plasma and NE-Ca of TRAMP mice gavage-treated with AGN (5 mg/mouse) vs. equimolar D/DA (3 mg/mouse). **A.** Chemical structures of D, DA and DOH. Arrow width depicts greater D to DOH conversion than does DA *in vivo*. **B**. Represenative LC-MS chromatograms of separation of DOH, D and DA in a NE-Ca sample. Note the different mass intensity scales for DOH vs. D and DA tracings. **C**. Plasma concentrations and NE-Ca content of D, DA and DOH in TRAMP mice gavage-treated daily from 8 to 16 and 28 weeks of age. Blood and tumors were collected at 3 hours after the last dose. ANOVA of plasma DOH data indicated a significant effect of length of gavage, but no effect of forms of supplement (AGN vs. D/DA).

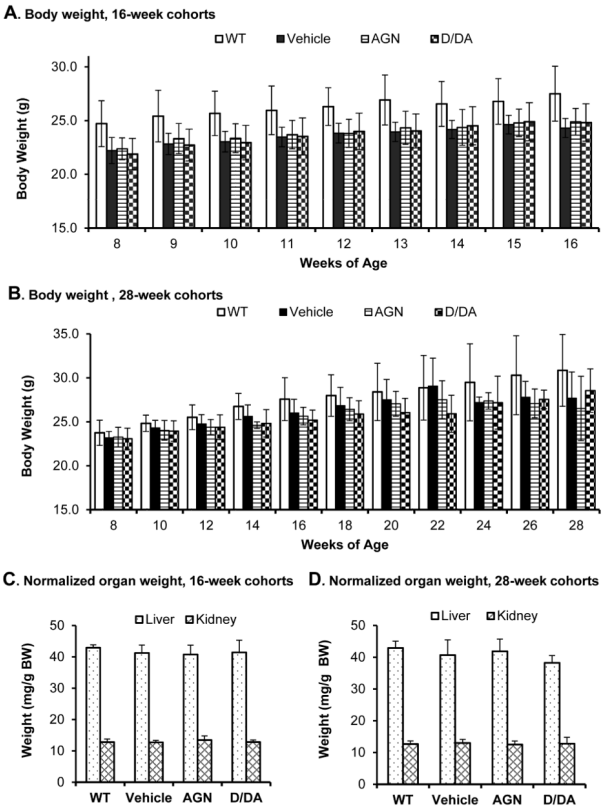

Figure 2.

Effects of AGN and D/DA on body weight and organ weight. WT, wild type vehicle; Vehicle, TRAMP mice treated by excipient vehicle; AGN, TRAMP mice treated with AGN; D/DA, TRAMP mice treated with D/DA. **A**. Body weight of 16-week cohorts. **B**. Body weight of 28-week cohorts. **C**. Normalized organ weight of 16-week cohorts. **D**. Normalized organ weight of 28-week cohorts. Animal numbers: 16-week cohorts: WT, n=6; Vehicle (TRAMP), n=13; AGN (TRAMP), n=11; D/DA (TRAMP), n=11. 28-week cohorts, WT, n=8; Vehicle (TRAMP), n=20, AGN (TRAMP), n=21 and D/DA (TRAMP), n=22, respectively. Mean ± SD.

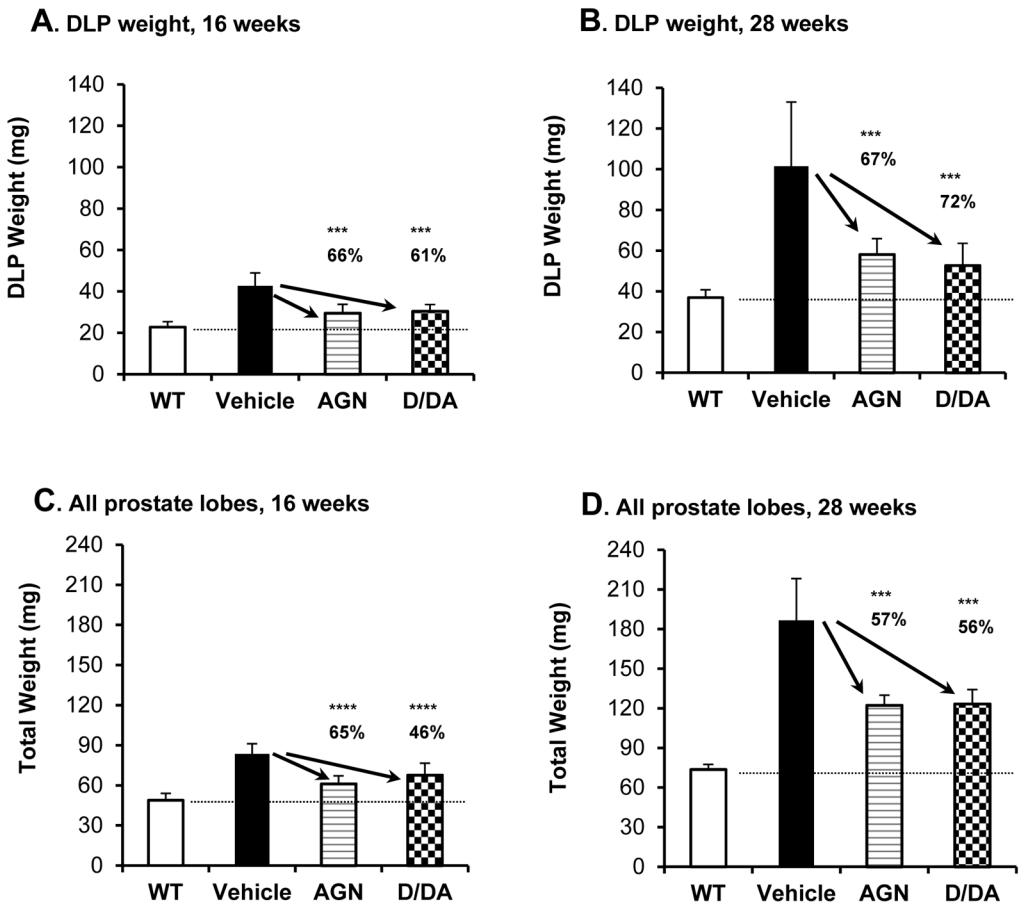

Figure 3.

Effects of daily gavage-administered AGN vs. D/DA on dorsolateral prostate lobe weight and total prostate weight. **A**. DLP weight at 16 weeks. **B**. DLP weight at 28 weeks. **C**. Total prostate weight at 16 weeks. **D**. Total prostate weight at 28 weeks. TRAMP mice bearing NE tumors were excluded from 28-week due to distinct lineages. Mean ± SD. Number of mice: 16-week cohorts, WT, n=6, Vehicle (TRAMP), n=13, AGN (TRAMP), n=11 and D/DA (TRAMP), n=11, respectively. 28-week cohorts, WT, n=8, Vehicle (TRAMP), n=13, AGN (TRAMP), n=15 and D/DA (TRAMP), n=14, respectively. One-way ANOVA followed by the Dunnett post test, ***: P<0.001, ****: P<0.0001.

A. T-Ag and Ki-67 staining of dorsolateral prostate (28 weeks of age)

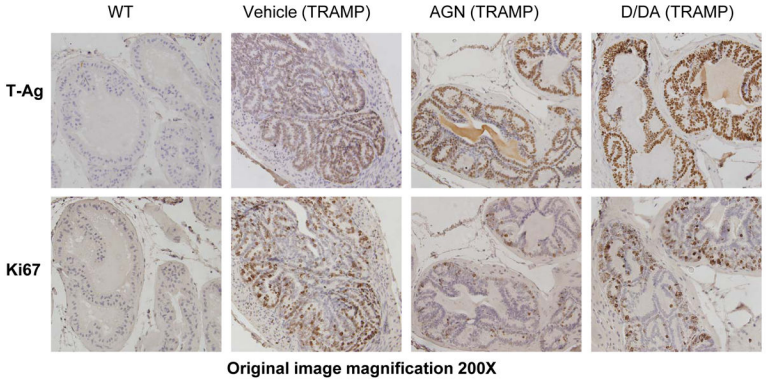

Original image magnification 200X

B. Lesion scores in dorsolateral prostate

Age killed	Group	Score
16 weeks	Vehicle	7.9±2.0
	AGN	6.2±1.6*
	D/DA	6.5±0.8
28 weeks	Vehicle	11.1±2.1
	AGN	7.9±1.6***
	D/DA	7.2±1.4***

C. mRNA measured by qRT-PCR in DLP

Gene	28-week Pooled DLP relative to wild type as 1		
	TRAMP Vehicle	TRAMP AGN	TRAMP D/DA
Hmgb2	3.31	2.38	2.14
p21	2.03	1.56	1.33
Ccna2	4.51	3.34	3.04
p16	21.52	15.25	14.3
Pcna	2.45	1.84	1.71

Figure 4.

Effects of AGN and D/DA on TRAMP dorsolateral prostate lession progression and associated cell cycle regulatory genes. **A.** Representative immunohistochemical analysis of SV40-T antigen (T-Ag) and Ki-67 expression in DLP. Magnification, 200×. Dark brown nuclear staining. **B**. Mean score of DLP lesions. 16 weeks, Vehicle (TRAMP), n=13; AGN (TRAMP) n=11; D/DA (TRAMP) n=10. 28 weeks, Vehicle (TRAMP), n=13; AGN (TRAMP) n=15; D/DA (TRAMP) n=14. **C**. Real time qRT-PCR analysis of mRNA levels in 28-week pooled DLP. One-way ANOVA followed by the Dunnett post test, *: P<0.05, **: P<0.01, ***: P<0.001.

A. Incidence of NE-Ca and lymph node metastasis

Age killed	Gavage	Total Mice	Mice with epithelial lesions only	Mice with NE-Ca	Mice with lymph node metastasis
16 weeks	Vehicle	13	13	0	0
	AGN	11	11	0	0
	D/DA	11	11	0	0
19-28 weeks	Vehicle	20	13	7	7
	AGN	21	15	6	3
	D/DA	22	14	8	3

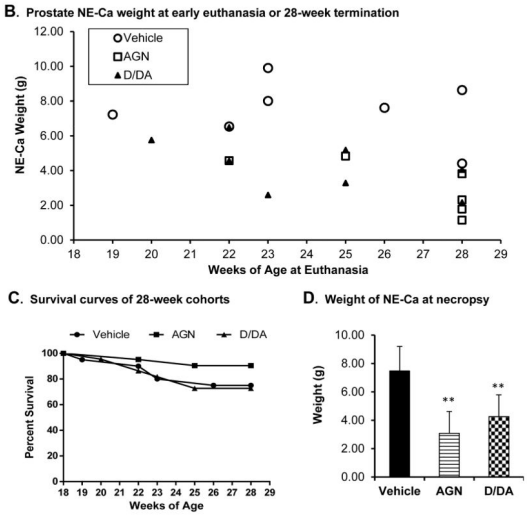

Figure 5.

Effects of AGN and D/DA on NE-Ca incidence, growth and metastasis. **A**. The incidence of NE tumors and metastatic lymph nodes in 16-week and 19–28-week cohorts. **B**. Weight of NE-Ca at euthanasia or terminal kill (28 weeks). **C**. Survival curves of 28-week TRAMP cohorts. Vehicle, n=20, AGN, n=21 and D/DA, n=22, respectively. **D.** Weight of NE-Ca. Vehicle (TRAMP), n=7, AGN (TRAMP), n=6 and D/DA (TRAMP), n=8, respectively. Mean ± SD, One-way ANOVA followed by the Dunnett post test, **: P<0.01.

Cancer Prev Res (Phila). Author manuscript; available in PMC 2016 September 01.

Table 1

Real time qRT-PCR analysis of mRNA levels in NE-Ca

Gene Symbol	Gene Name	Major function category	Relative to TRAMP Vehicle as 100%						
			TRAMP Vehicle	SD	TRAMP AGN	SD	TRAMP D/DA	SD	ANOVA *p-value*
Pcna	proliferating cell nuclear antigen (DNA repair)	Proliferation	100	15	39	9	51	19	0.001
Fen1	flap endonuclease 1 (PCNA complex, DNA repair)	Proliferation	100	20	47	12	53	18	0.001
Stat3	signal transducer and activator of transcription 3	Proliferation	100	40	27	3	48	27	0.008
Syt4	**synaptotagmin IV**	Neuron/NE	100	70	6	2	16	6	0.007
Sox5	**SRY (sex determining region Y)-box 5**	Neuron/NE	100	17	44	19	44	11	0.001
Fgfr1	fibroblast growth factor receptor 1	Angiogenesis	100	12	77	11	88	27	0.246
Fgf10	**fibroblast growth factor 10**	Angiogenesis	100	62	45	23	37	13	0.066
Fgfbp3	**fibroblast growth factor binding protein 3**	Angiogenesis	100	68	21	4	55	43	0.076
Mmp2	**matrix metallopeptidase 2**	Angiogenesis	100	43	41	19	34	8	0.005
Nos2	nitric oxide synthase 2, inducible	Angiogenesis	100	29	**52**	12	171	114	0.031
Vegf	vascular endothelial growth factor	Angiogenesis	100	32	**70**	24	115	30	0.046
Flt1	FMS-like tyrosine kinase 1 (VEGF receptor)	Angiogenesis	100	26	75	20	108	37	0.258
Snai2	**snail family zinc finger 2**	EMT-metastasis	100	63	23	6	45	51	0.089
Twist1	twist basic helix-loop-helix transcription factor 1	EMT-metastasis	100	33	**22**	5	98	53	0.008
Notch1	notch 1	EMT-metastasis	100	50	**46**	14	87	55	0.227
Tgfbr2	transforming growth factor, beta receptor II	EMT-metastasis	100	39	**48**	13	71	47	0.157
Mmp12	matrix metallopeptidase 12 (macrophage)	Invasion-metastasis	100	39	**38**	15	107	103	0.072
E- cadherin	cadherin 1 (epithelial specific)	Epithelium	100	116	**233**	122	116	129	0.039
Vpp1	**ventral prostate predominant 1**	Epithelium-prostate specific	100	52	3088	2823	1916	2124	0.001
Cpa3	**carboxypeptidase A3, mast cell**	Inflammation	100	56	29	19	31	31	0.027
Cma1	chymase 1, mast cell	Inflammation	100	54	**24**	9	60	53	0.073
Mcpt6	mast cell protease 6	Inflammation	100	52	**18**	5	60	49	0.068
Il6st	interleukin 6 signal transducer	Inflammation	100	16	61	7	66	24	0.009
Rela	v-rel reticuloendotheliosis viral oncogene homolog A	Inflammation	100	18	**59**	12	102	25	0.010
uPa	plasminogen activator, urokinase	Invasion	100	33	80	31	73	30	0.467

TRAMP Vehicle, n=4, TRAMP AGN, n=4 and TRAMP D/DA, n=4, respectively. Gene names in **bold** denote those commonly affected by AGN and D/DA; Bold numbers in AGN column denote those affected only by AGN.